

*Original Research*

# Adsorption of VOCs onto Single Vacancy Defected Germanene Monolayer: a Study on Their Structure and Electronic Properties by DFT Calculations

Hieu Trung Nguyen<sup>1\*</sup>, Van On Vo<sup>2</sup>

<sup>1</sup>Institute of Applied Technology, Thu Dau Mot University, 06 Tran Van On Street, Phu Hoa Ward, Thu Dau Mot City 750000, Binh Duong Province, Vietnam

<sup>2</sup>Big Data and Data Analytics Group, Center for Forecasting Study, Thu Dau Mot University, 06 Tran Van On Street, Phu Hoa Ward, Thu Dau Mot City 750000, Binh Duong Province, Vietnam

*Received: 13 January 2023*

*Accepted: 17 April 2023*

## Abstract

The two-dimensional germanene material is one of the potential candidates for sensor applications for gases such as VOCs due to its unique structural and electronic properties. The fabrication of these materials is practically not free from defects in the material. Therefore, to better understand the structural and electronic properties of this material when adsorbing VOCs, this study performed DFT calculations of single vacancy-defected monolayer germanene when adsorbing molecules such as acetone, propanol, and toluene. These DFT calculations took into account the intermolecular Van der Waal interactions between germanene and the adsorbed gases. The model of the germanene monolayer is a 4×4 supercell lacking a Ge atom with a distance between the two layers of 30 Å. The results show that the single vacancy-defected monolayer germanene has two stable configurations with a not-too-large difference in energy. Adsorption of molecules such as acetone, propanol, and toluene onto these monolayers is physisorption (adsorption energies in the range of -0.205 eV to -0.421 eV), however, they also affect the structural and bandgap properties of these monolayers. The bandgap change of the systems in the presence of these adsorptions is not as large (bandgap changes in about 3 meV - 40 meV) as chemical adsorption. Frontier orbitals such as HOMO (highest occupied molecular orbital) and LUMO (lowest unoccupied molecular orbital) of the VOCs are located quite far from the Dirac points (Fermi level) of the defected germanenes. The negative charge transfer from the defected germanenes to the VOC molecules decreases in the order: Ge31A-Ace > Ge31A-Pro>Ge31B-Ace>Ge31A-Tol

---

\*e-mail: hieunt@tdmu.edu.vn

>Ge31B-Prol>Ge31B-Tol. The signals of this small change will help in determining the type and concentration of these gases when applying these monolayers as sensors.

**Keywords:** 2D Germanene materials, VOCs adsorption, vdW-DFT, single vacancy-defected monolayer

## Introduction

VOCs (volatile organic compounds) are considered air pollutants and seriously affect human health. Researchers are constantly looking for ways to limit their emissions into the environment and eliminate them using a variety of methods [1]. However, techniques for detecting their presence in the air with high sensitivity and reliability are needed before their removal can be considered. In addition, certain human body cells also emit VOCs when people have certain diseases such as cancer [2]. VOC sensors are one of the methods to quickly diagnose the condition of these diseases with advantages such as being fast, accurate, non-invasive, easy to perform, etc. [3]. Therefore, the research and development of these VOC sensors are very meaningful in practice. Besides, the VOCs in the air can be treated by many different methods, including adsorption [4-6]. And the main mechanism of VOC sensors is also based on the changes in the physical and chemical properties of the materials during the adsorption of these VOCs onto their surface [7]. Accordingly, practical application studies need to have basic orientations from theoretical studies on the adsorption of VOCs on potential sensor materials and adsorbents.

The materials commonly used in theoretical research on the adsorption of VOCs are two-dimensional materials of the graphene family such as graphene, silicene, and germanene [8]. Graphene is the first successfully fabricated material in this family with properties such as high surface area, low electrical noise, and extremely mobile electrons [9]. But the disadvantage of graphene is its low selectivity due to the adsorption of even common gases in the air. [10]. Silicene and germanene have also been successfully fabricated in practice recently and have the same precious properties as graphene such as high electron mobility, magnetism, semi-metallic, quantum hall effect, etc. [11]. However, these precious properties are not shown when silicene is coated onto the metal substrate. Unlike the planar structure of the graphene layer, silicene and germanene have a buckled honeycomb structure [12]. This gives them a higher chemical reactivity and stronger adsorption of gas molecules than graphene [13]. If many theoretical studies on the adsorption of gas molecules on silicene have been done, those of germanene has not yet been performed commensurate with its potential. Therefore, in this study, we chose germanene as a research object to contribute to a deeper understanding of its properties.

When the human body is exposed to VOCs, it can cause diseases of the sensory system, nervous system, cancer, etc. [14-17]. In terms of current practice, VOCs

are quantified and identified only by expensive gas chromatographic systems with complicated and time-consuming operating procedures [18]. Therefore, the detection of VOCs with two-dimensional materials such as germanene opens up promising new application prospects. Indoor VOCs are generally classified into three main categories: aromatic hydrocarbons, chlorocarbons, and other organic solvents [19]. There are about 20 popular VOCs commonly detected in indoor environments, with acetone in the top position [20]. In addition, in the list of these 20 VOCs, there are other compounds such as propanol, toluene, etc. Since the calculation of the adsorption of all these 20 VOCs onto germanene is very time-consuming and impractical, we only selected three typical VOCs, acetone, propanol, and toluene as the research objects within the scope of this work.

Recent studies show that germanene is an ideal material for gas adsorption and gas sensors for some common gases. The DFT study for the adsorption of gases such as  $N_2$ , CO,  $CO_2$ ,  $H_2O$ ,  $NH_3$ , NO,  $NO_2$ , and  $O_2$  was performed by Xia Wenqi et al. [21]. Gases such as  $N_2$ , CO,  $CO_2$  and  $H_2O$  are physically adsorbed onto germanene, while gases such as  $N_2$ , CO,  $CO_2$  and  $H_2O$  are chemically adsorbed onto germanene. The moderate adsorption of gases such as  $NH_3$  and NO makes germanene a possible sensor for these two gases. Another study conducted DFT calculations for the adsorption of liver cirrhosis VOCs such as methanol, 2-pentanone, and limonene onto bare and hydrogenated germanene nanosheets [22]. The authors found that liver cirrhosis VOCs are physically adsorbed onto germanene nanosheets, which makes them easier to desorption and helps to achieve the reversibility of biosensors from germanene nanosheets. However, fabricating two-dimensional materials such as germanene in practice will inevitably present defects in their structure, and to the best of our knowledge, there is currently no theoretical study on the adsorption of VOCs onto single vacancy defected germanene monolayer. Therefore, this work investigates the structural and electronic properties of a single vacancy-defected germanene monolayer before and after the adsorption of VOCs such as acetone, propanol, and toluene.

## Material and Methods

### Model Building

The single-cell germanene monolayer was built using Avogadro 1.2.0 software with structure parameters such as buckling parameters, bond lengths,

bond angles, and lattice cell parameters referenced from published works in the literature. The germanene monolayer supercell  $4\times 4$  was built from its single cell using Vesta 3.5.8 software with a distance between the two layers of 30 Å to eliminate interactions between them. Molecules of VOCs such as acetone, propanol, and toluene have been constructed using Avogadro 1.2.0. Systems containing germanene monolayer and VOC were built using Vesta 3.5.8.

### Computational Methodology

The Vienna Ab Initio Simulation Package (VASP 6.1.0) with PAW potential was used for all computations that utilized the generalized gradient approximation (GGA) and density functional theory [23, 24]. The Van der Waals interaction was taken into account in all computations by using the PBE-vdW functional to create the findings in better agreement with the experiment [25] since the Van der Waals functionals are predicted to be better than van der Waals correction schemes [26, 27]. When this DFT calculation was tested as a benchmark, it showed good agreements between experiments and calculations in the case of graphene. A cutoff energy of 450 eV was employed for the plane-wave basis set. A  $7\times 7\times 1$  gamma-centered k-point mesh was utilized to yield energy convergence in geometric optimization, but that of  $13\times 13\times 1$  was set in static total energy and band structure calculation. The highest Hellmann-Feynman force acting on each atom was reduced to less than 0.01 eV/Å for all configurations. The stable configurations of single-vacancy defected germanene are denoted as Ge31A and Ge31B, respectively, while systems consisting of these two configurations and molecules such as acetone, propanol, and toluene are denoted as Ge31A-Ace, Ge31B-Ace, Ge31A-Prol, Ge31B-Prol, Ge31A-Tol, and Ge31B-Tol, respectively.

## Results and Discussion

### The Geometrical Structures of Single-Vacancy Defected Germanene Monolayer

The single-vacancy defected germanene monolayer model was constructed by removing a Ge atom from the perfect  $4\times 4$  germanene supercell. According to [28], for single-vacancy defected germanene, two stable structures need to be considered for investigation. For configuration A (Figs 1(b, e)), 12 Ge atoms around the single-vacancy defect (indexes of 2, 6, 7, 10, 11, 12, 18, 19, 22, 23, 26, and 27) collapse into a non-planar 12-edge polygon. For configuration B (Figs 1(c, f)), a Ge atom (index of 7) moves into the center of the single-vacancy defect and forms two hexagons and two pentagons (indexes of 2, 3, 6, 8, 10, 11, 12, 18, 19, 20, 22, 23, 26, and 27) or a non-planar polygon with 14 edges and one central point. These two configurations

were initially approximated manually using the vesta 3.5.8 software and then optimized for structure and energy using the method described above. The results show that they have almost the same geometrical and energetic stability with a system energy difference of about 0.1 eV; in which, configuration B is more stable than configuration A but the difference is not high. Configuration A has the distances of the Ge6-Ge7, Ge7-Ge11, and Ge11-Ge6 pairs of 3.582 Å, 3.628 Å, and 3.559 Å, respectively; while the bond angles of Ge18Ge6Ge22, Ge19Ge7Ge23, and Ge26Ge11Ge27 are 99.524°, 100.249°, and 98.925°, respectively. Configuration B has the distances of Ge6-Ge11, Ge11-Ge23, Ge23-Ge19, Ge19-Ge6, Ge6-Ge7, Ge11-Ge7, Ge19-Ge7, and Ge23-Ge7 pairs of 3.779 Å, 4.304 Å, 3.937 Å, 4.573 Å, 3.478 Å, 3.053 Å, 2.671 Å, 2.597 Å, respectively; the bond angles of Ge6Ge7Ge11, Ge11Ge7Ge23, Ge23Ge7Ge19, and Ge19Ge7Ge6 are 70,358°, 98,915°, 96.713°, and 95.179°, respectively. Because germanene does not have a planar layered structure like graphene, the single-vacancy defects of both configurations A and B are not highly symmetric.

The optimization of the geometry and energy of single-vacancy defected germanene and VOC systems by the above calculation method have been performed many times to find the most stable configurations. In the beginning, the VOC molecule is randomly placed on top of the single-vacancy defected germanene 3.50 Å from the lowest atom of the VOC molecule. Because the site of single-vacancy defects has a high potential due to the instability of the defect, VOC molecules are preferentially placed at the center of these defects. The most stable configurations of each defected germanene and VOC system are illustrated in Fig. 2.

### Binding Energy

The binding energies of the defected germanene, i.e., Ge31A and Ge31B configurations, have values of -68.557 eV and -68.670 eV, respectively (Table 1). The difference in binding energy values of these two configurations is 113 meV. In terms of geometrical structure, these two configurations have a slight difference mainly in the position of the Ge7 atom. Specifically, the distances between the Ge7-Ge6, Ge7-Ge11, Ge7-Ge19, and Ge7-Ge23 pairs in the Ge31A structure are 3.582 Å, 3.628 Å, 2.566 Å, and 2.562 Å, respectively; meanwhile, the distances between these pairs in the structure of Ge31B are 3.478 Å, 3.053 Å, 2.671 Å, and 2.597 Å, respectively. We can see that the Ge7 atom in the Ge31B structure is closer to the Ge6 and Ge11 atoms and further away from the Ge19 and Ge23 atoms than that in the structure of Ge31A. If considered on the same system of defected germanene and VOC, i.e., with the same number and type of element, the variation of the calculated binding energies also shows different trends. For two systems Ge31A-Ace and Ge31B-Ace, the binding energy of the Ge31A-Ace system is lower than that of the

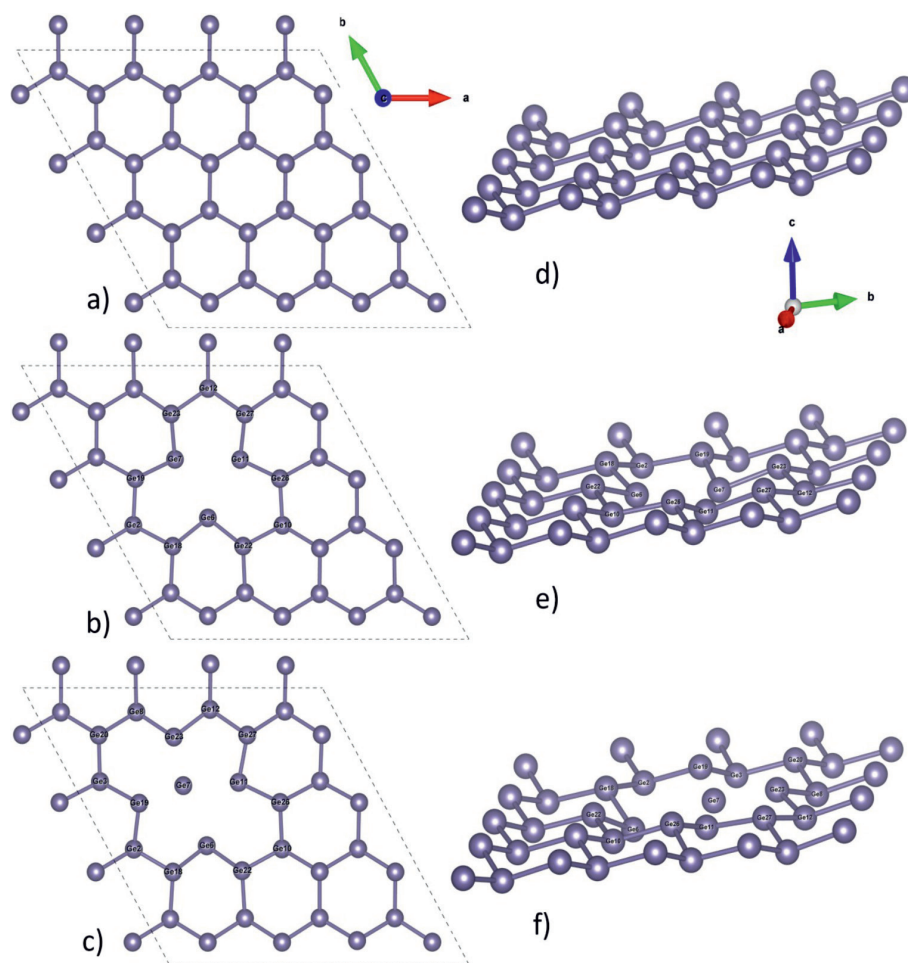


Fig. 1. The perfect germanene (a, d) and possible structures of single-vacancy defected germanene: structure A with 12 indexed Ge atoms of non-flat 12 edges polygon (b, e) and structure B with 16 indexed edge Ge and a center Ge atoms of non-flat 16 edges polygon (c, f).

Ge31B-Ace system 46 meV, i.e., the contrast trend in binding energies of Ge31A and Ge31B. This can be explained because the adsorption energy of acetone on Ge31B is quite low (-0.205 eV). However, for the two systems Ge31A-Prol and Ge31B-Prol, the trend of their binding energies is similar to that of Ge31A and Ge31B, i.e. configuration B will be more energetically and structurally stable than configuration A. It can be explained that the adsorption energy of propanol in these two configurations is not much different, so the trend of binding energies of the substrate remains the same. The same conclusion is obtained for the trend of binding energies of the two systems Ge31A-Tol and Ge31B-Tol and can be explained with the same reason that the adsorption energies are not too different.

#### Adsorption Energy Profile

The adsorption energy of the VOC onto the defected germanene is calculated by the difference in binding energies of the optimized VOC/defected germanene system and when the VOC of this system is moved far enough away from the defected germanene to eliminate

their interaction. Therefore, these adsorption energies can be calculated using the following formula:

$$E_a = E_{VOC/defected\ germanene} - E_{saturation} \quad (1)$$

Where  $E_a$  is the adsorption energy of VOC on defected germanene,  $E_{VOC/defected\ germanene}$  is the energy of the VOC and defected germanene system that has been optimized in geometry and energy,  $E_{saturation}$  is the energy of the VOC and defected germanene system when VOC is far enough away from defected germanene to eliminate interactions between them. Equation (1) above can be transformed into the following equation:

$$E_a = E_{VOC/defected\ germanene} - E_{VOC} - E_{defected\ germanene} \quad (2)$$

Where  $E_{VOC}$  and  $E_{defected\ germanene}$ , respectively, the binding energies of the VOC molecule and the defected germanene monolayer have been optimized in terms of geometry and energy.

The adsorption energies of VOCs on defected germanenes (Table 1) are ranked in descending order

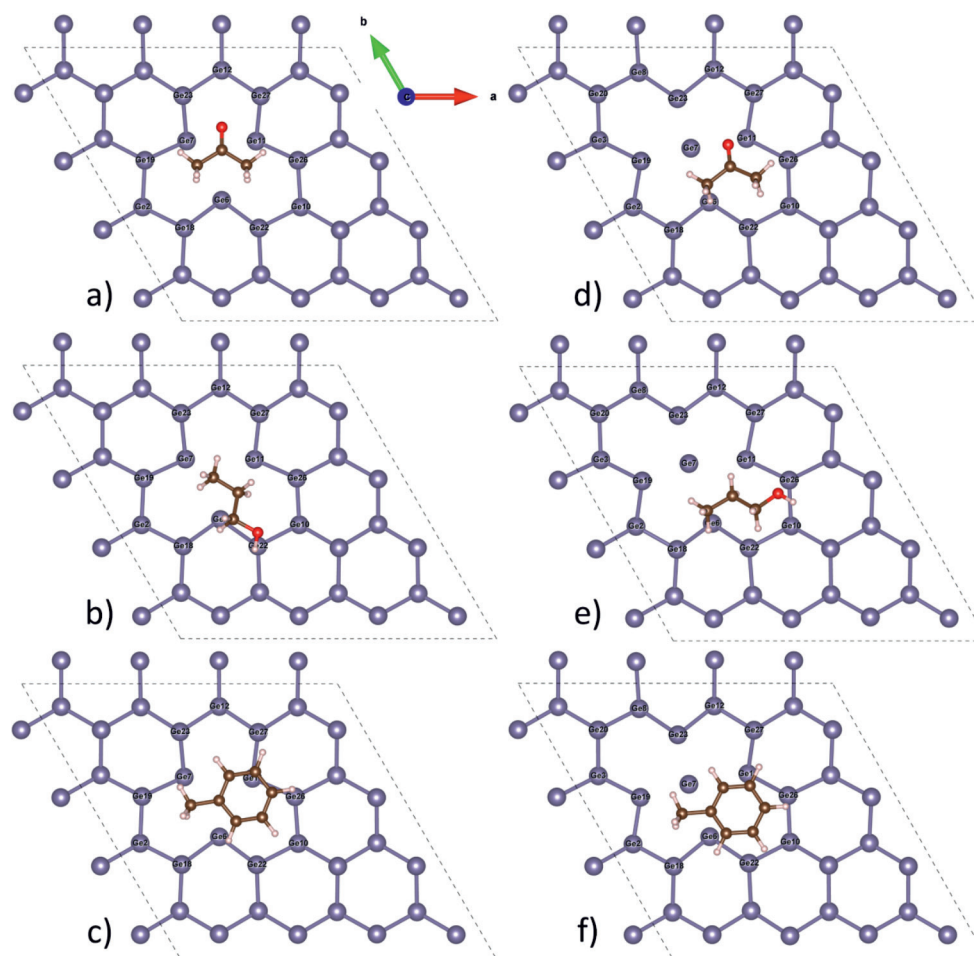


Fig. 2. The most stable structures of Ge31A-Ace a), Ge31A-Prol b), Ge31A-Tol c), Ge31B-Ace d), Ge31B-Prol e), and Ge31B-Tol (f).

Table 1. Binding energies ( $E_0$ ), adsorption energies ( $E_a$ ), charge transfer from defected germanene to VOC, distances from the lowest atom of VOC to defected germanene, bandgaps ( $E_g$ ) at Dirac point of defected germanene.

Model	Binding energy (eV)	Adsorption energy (eV)	Charge transfer (e)	Distance (Å)	Bandgap (meV)
Ge31A	-68.557	x	x	x	40.2
Ge31B	-68.670	x	x	x	41.1
Ge31A-Ace	-118.828	-0.322	-0.083	3.400	37.4
Ge31A-Prol	-126.290	-0.298	-0.076	3.317	52.0
Ge31A-Tol	-151.352	-0.421	-0.061	3.222	26.7
Ge31B-Ace	-118.782	-0.205	-0.069	3.355	x
Ge31B-Prol	-126.422	-0.344	-0.057	3.115	44.0
Ge31B-Tol	-151.371	-0.347	-0.051	3.238	54.5

Note: x indicates non-existence

of interaction strength as follows: Ge31A-Tol>Ge31B-Tol>Ge31B-Prol>Ge31A-Ace>Ge31A-Prol>Ge31B-Ace. These adsorption energies are in the low-medium range and are therefore classified as physical adsorption. Consider the case of the toluene molecule, since this molecule is composed of more atoms and contains

conjugated  $\pi$  bonds, it causes a significantly stronger interaction with the defected germanene. Because germanene also contains conjugated  $\pi$  bonds, the  $\pi$ - $\pi$  interaction is the major contributor to the adsorption energy of toluene. The physical adsorption for the acetone and propanol molecules is mainly due to

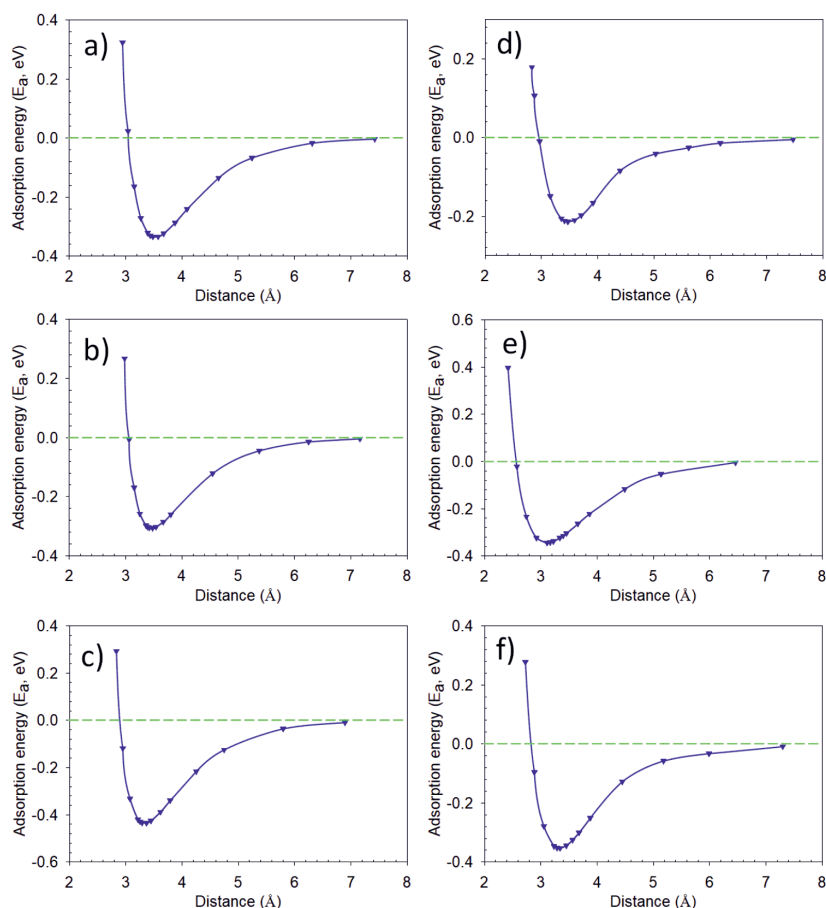


Fig. 3. Interaction energy profiles of Ge31A-Ace a), Ge31A-Prol b), Ge31A-Tol c), Ge31B-Ace d), Ge31B-Prol e), and Ge31B-Tol systems.

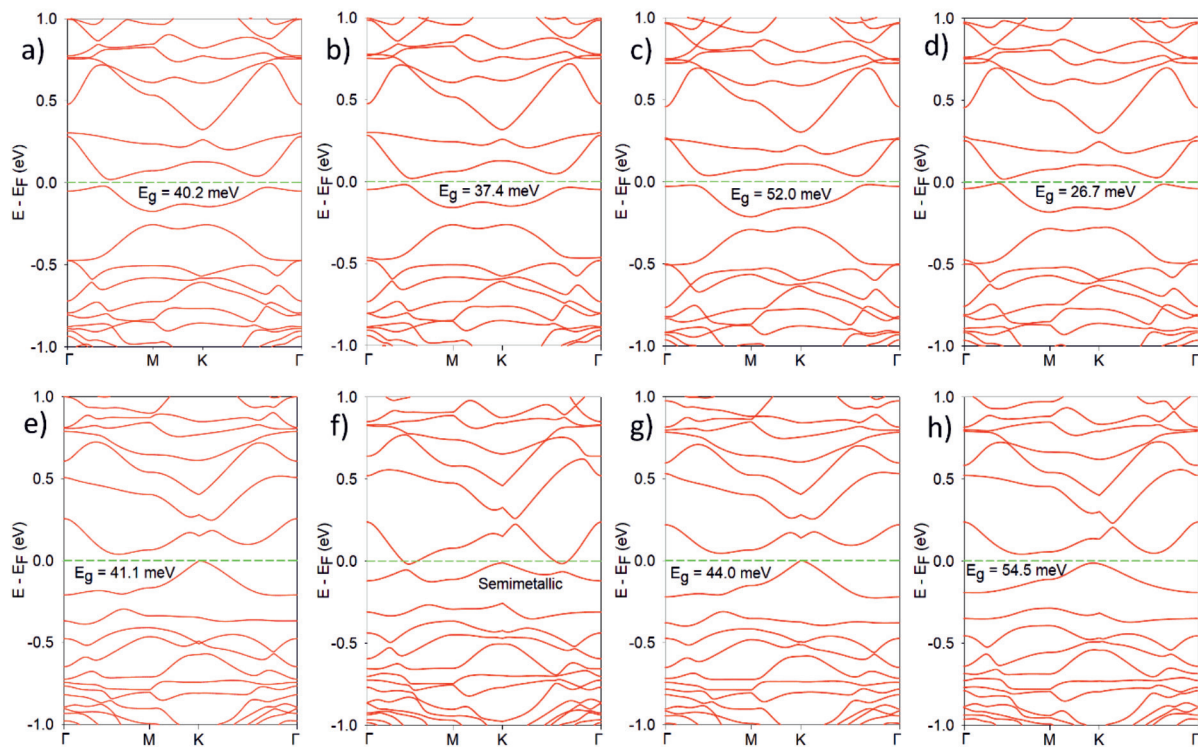


Fig. 4. Electronic band structures of Ge31A (a), Ge31A-Ace (b), Ge31A-Prol (c), Ge31A-Tol (d), Ge31B (e), Ge31B-Ace (f), Ge31B-Prol (g), and Ge31B-Tol (h) systems. The green dotted line denotes the Fermi level, which is set to zero.

the intermolecular Van der Waal interaction between the VOC and the defected germanene. Except for the case of Ge31B-Ace with relatively low adsorption energy, the systems Ge31A-Ace, Ge31A-Prol, and Ge31B-Prol do have not much different adsorption energies. This low adsorption energy difference can be explained by the similar number of atoms and structures of these two molecules. The interaction energy varies with the distance between the VOC and the defected germanene as illustrated in Fig. 3. In general, the changing trend of this interaction is the same but only slightly different at the distance where the interaction energy is minimized. (adsorption energy). At the distance between the VOC and the defected germanene less than 3 Å, a repulsive force exists between them, represented by the positive interaction energy. When moving VOC molecules from the energy minimum position away from the germanene surface, their interaction energies become weaker but still have a negative value. However, when the distance between them is about 7 Å, there is almost no interaction force between them.

## Electronic Properties

The electronic band structures of defected germanenes and their systems with VOCs are illustrated in Fig. 4. Band structures of all these systems fall into the category of the indirect bandgap. Bandgaps of the two configurations Ge31A and Ge31B have nearly equivalent values (Table 1). These two bandgap values are higher than thermal fluctuations at room temperature (25 meV) due to the influence of vacancy defects [29]. As mentioned above, the adsorption of these VOCs on defected germanene is physical adsorption, so the bandgap change of the systems in the presence of this adsorption is not as large (bandgap changes in about 3 meV-40 meV) as chemical adsorption. It can be noticed that in some cases (Ge31A-Ace, Ge31A-Tol, Ge31B-Ace) the bandgaps of the systems are lower than that of Ge31A and Ge31B; this could be explained by VOC adsorption which stabilized the electronic structure of defected germanene. For the remaining cases (Ge31A-Prol, Ge31B-Prol, Ge31B-Tol), the bandgap was opened

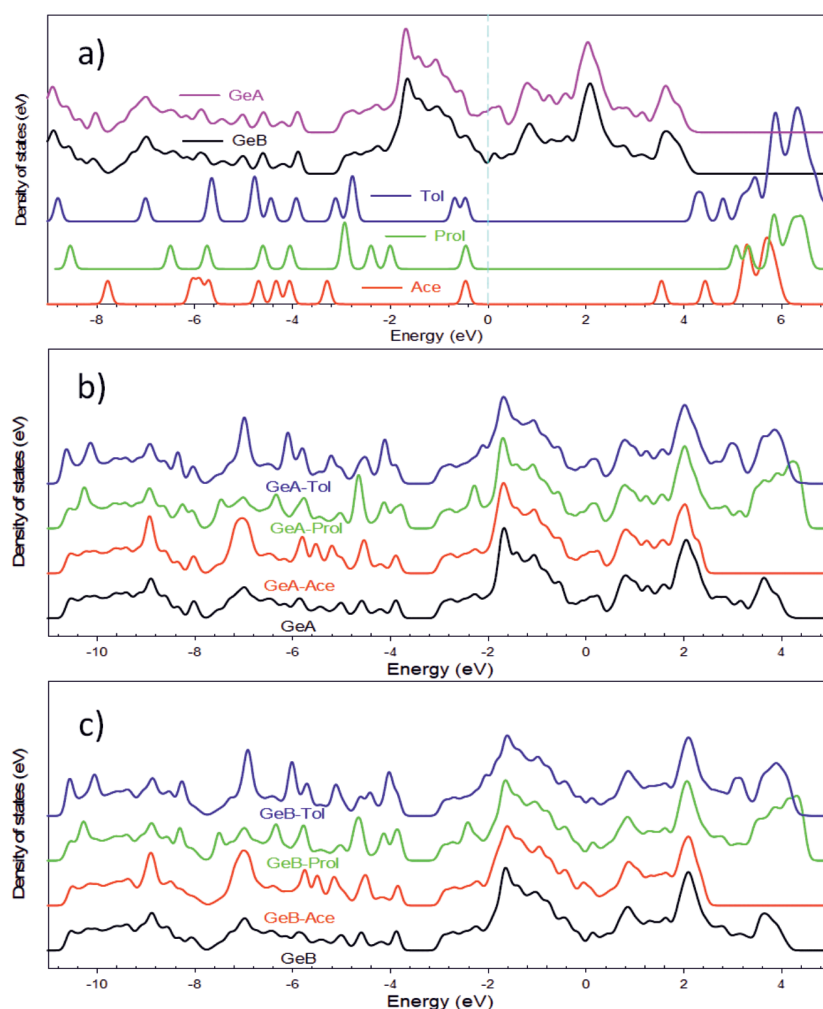


Fig. 5. Density of states (DOS) of acetone, propanol, toluene, Ge31A, Ge31A-Ace, Ge31A-Prol, Ge31A-Tol, Ge31B, Ge31B-Ace, Ge31B-Prol, and Ge31B-Tol. Other molecules are compared to the vacuum level of defected germanene, with the Fermi level of defected germanene set to zero.

from 3 meV to 13 meV; in general, they all have higher adsorption energies.

The densities of states (DOS) of the investigated VOCs and systems are illustrated and compared in Fig. 5. We can see that frontier orbitals such as HOMO (highest occupied molecular orbital) and LUMO (lowest unoccupied molecular orbital) of the VOCs are located quite far from the Dirac points (Fermi level) of the defected germanenes. These molecules, therefore, have low reactivity towards defected germanene leading to physisorption rather than chemisorption. [30] This can be explained by the large radius and low electronegativity of the Ge elements. And because of the weak interaction, the DOS of the VOC and defected germanene systems are not much different from the pristine defected germanene's DOS (Fig. 5(b, c)).

### Charge Transfer and Charge Density Difference

When adsorption takes place, both physically and chemically, there is a partial charge transfer between the adsorbent and the adsorbate. According to Table 1, the

negative charge transfer from the defected germanenes to the VOC molecules decreases in the order: Ge31A-Ace > Ge31A-Prol > Ge31B-Ace > Ge31A-Tol > Ge31B-Prol > Ge31B-Tol. This is understandable since germanenes have highly mobile and dense conjugated  $\pi$  electrons, so it will be delivered to the adsorbed VOC molecules. However, this charge transfer is not very large due to the nature of weak physical adsorption interactions. [31] Among them, the toluene molecule receives the least negative charge compared to acetone and propanol due to its high conjugated  $\pi$  electron density. The acetone molecule gets the most negative charge from defected germanene because its molecular structure contains less hydrocarbons and is more polarized than propanol. From Figs 6 and 7, it can be seen that the charge transfers from the germanene substrate to the doping part (VOCs). This can be explained by the more electron-rich structure in the conduction band of the germanene substrate compared to the doping parts. The electrons of the doping parts are mainly located in the low-energy valence band, so no charge transfer from the doping parts to the germanene substrate is possible.

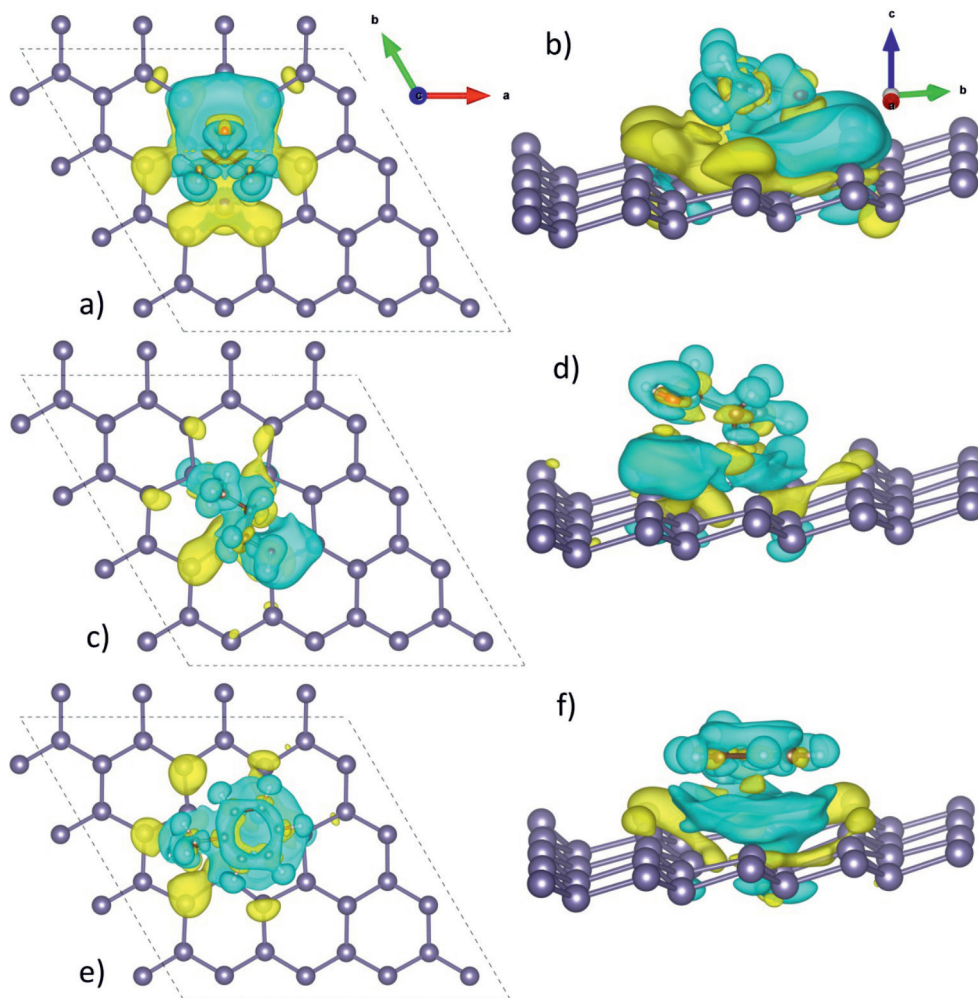


Fig. 6. Charge density differences of Ge31A-Ace (a, b), Ge31A-Prol (c, d), and Ge31A-Tol (e, f) systems. (Blue regions indicate increased charge density upon VOC adsorptions, while yellow regions indicate decreased charge density).

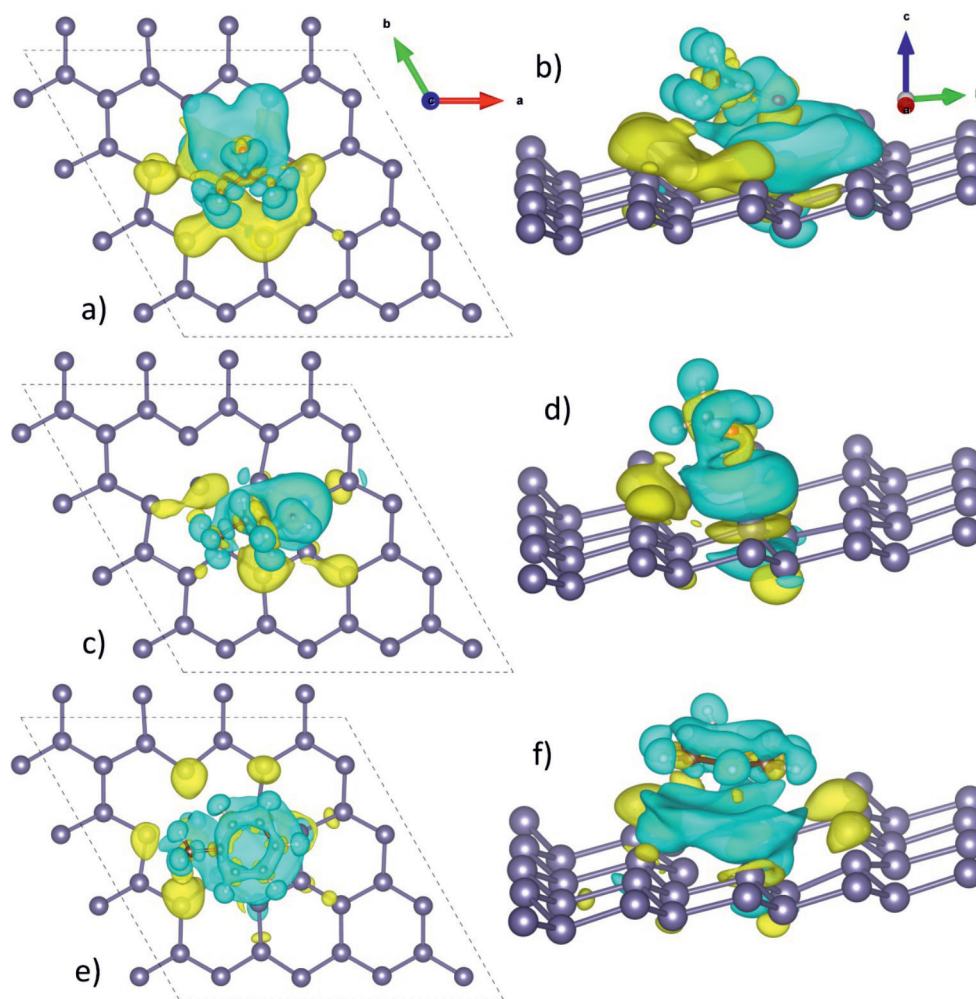


Fig. 7. Charge density differences of Ge31B-Ace (a, b), Ge31B-Prol (c, d), and Ge31B-Tol (e, f) systems. (Blue regions indicate increased charge density upon VOC adsorptions, while yellow regions indicate decreased charge density).

This charge transfer is the main cause of the physical adsorption interaction between the germanene substrate and the VOCs.

For the charge density difference, the illustrations (Figs 6, and 7) will help us to understand more deeply about the nature of the orbitals interactions of the adsorbent and adsorbate [32]. In Fig. 6(a, b), we can see a strong main interaction between the p-orbital of the oxygen atom and the p orbital system around the vacancy-defect point. However, in the case of propanol (Fig. 6(c, d)), it is the predominant interaction of the s-orbital of the hydrogen atom and the p-orbital system around the vacancy-defect point; therefore, the charge transfer in this case is lower compared to that of acetone. For the case of toluene (Fig. 6(e, f)), it is the repulsive interaction of the p-orbitals of toluene and the p-orbitals around the vacancy defect point on germanene; therefore, the charge transfer in this case is the lowest. Similar conclusions about charge transfer and orbital interactions were also obtained for the Ge31B-Ace, Ge31B-Prol, and Ge31B-Tol systems (Fig. 7).

## Conclusions

In summary, we investigated the adsorption of VOCs molecules such as acetone, propanol, and toluene onto the single-vacancy defected germanene monolayer using DFT-based calculations. The results show that there are two stable configurations of defected germanene, in which configuration B is slightly more stable than configuration A. Because the energy difference between these two configurations is not too large (113 meV), we calculated the adsorption of VOC molecules onto both of these configurations. The calculated adsorption energy is in the range -0.205 eV to -0.421 eV and is the physical adsorption with decreasing adsorption in the order: Ge31A-Tol>Ge31B-Tol>Ge31B-Prol>Ge31A-Ace>Ge31A-Prol>Ge31B-Ace. After the adsorption process, the Ge31A-Ace, Ge31A-Tol, and Ge31B-Ace systems have a reduction in bandgap compared to pristine defected germanene; while the Ge31A-Prol, Ge31B-Prol, and Ge31B-Tol systems have increased bandgap compared to the pristine defected germanenes. The weak physical

interaction nature of these adsorptions is demonstrated by the electronic band structures and DOS of the investigated systems. The process of transferring negative charge from defected germanene to VOCs molecules decreases in the order: Ge31A-Ace>Ge31A-Prol>Ge31B-Ace>Ge31A-Tol>Ge31B-Prol>Ge31B-Tol. This charge transfer is better understood through illustrations of the charge density difference of the investigated systems.

### Acknowledgments

This research is funded by Thu Dau Mot University, Binh Duong Province, Vietnam under grant number DT.21.1-056.

### Conflict of Interest

The authors declare no conflict of interest.

### References

- VAN TRAN V., PARK D., LEE Y.C. Indoor air pollution, related human diseases, and recent trends in the control and improvement of indoor air quality. *International Journal of Environmental Research and Public Health*, **2020**.
- HAKIM M., BROZA Y.Y., BARASH O., PELED N., PHILLIPS M., AMANN A., HAICK H. Volatile organic compounds of lung cancer and possible biochemical pathways. *Chemical Reviews*, **2012**.
- MAKARAM P., OWENS D., ACEROS J. Trends in Nanomaterial-Based Non-Invasive Diabetes Sensing Technologies. *Diagnostics*, **4** (2), **2014**.
- ZABIEGAŁA B. Organic compounds in indoor environments. *Polish Journal of Environmental Studies*, **2006**.
- WARDENCKI W., CURYŁO J., NAMIEŚNIK J. Green chemistry - Current and future issues. *Polish Journal of Environmental Studies*, **2005**.
- WENDA-PIESIK A. Volatile organic compound emissions by winter wheat plants (*Triticum aestivum* L.) under Fusarium spp. Infestation and various abiotic conditions. *Polish Journal of Environmental Studies*, **20** (5), **2011**.
- YIN F., YUE W., LI Y., GAO S., ZHANG C., KAN H., NIU H., WANG W., GUO Y. Carbon-based nanomaterials for the detection of volatile organic compounds: A review. *Carbon*, **2021**.
- TANG X., DU A., KOU L. Gas sensing and capturing based on two-dimensional layered materials: Overview from theoretical perspective. *Wiley Interdisciplinary Reviews: Computational Molecular Science*, **8** (4), **2018**.
- FU W., JIANG L., VAN GEEST E.P., LIMA L.M.C., SCHNEIDER G.F. Sensing at the Surface of Graphene Field-Effect Transistors. *Advanced Materials*, **2017**.
- LEE E., VAHIDMOHAMMADI A., LEE D., YOON J., BEIDAGHI M., YOON Y.S., KIM D.-J. Development in Two-Dimensional Nanomaterials for Wearable Health Monitoring Systems. *ECS Meeting Abstracts*, **MA2019-01** (44), **2019**.
- YOU Y., YANG C., ZHANG X., LIN H., SHI J. Emerging two-dimensional silicene nanosheets for biomedical applications. *Materials Today Nano*, **2021**.
- JOSE D., DATTA A. Structures and chemical properties of silicene: Unlike graphene. *Accounts of Chemical Research*, **47** (2), **2014**.
- ACUN A., ZHANG L., BAMPOULIS P., FARMANBAR M., VAN HOUSELT A., RUDENKO A.N., LINGENFELDER M., BROCKS G., POELSEMA B., KATSNELSON M.I., ZANDVLIET H.J.W. Germanene: The germanium analogue of graphene. *Journal of Physics Condensed Matter*, **2015**.
- LIANG R., ZHANG R., WEN H., MO J., HUANG M., CHEN H. Effects of Volatile Organic Compounds (VOCs) of *Cinnamomum burmannii* in Its Natural State on Physical and Mental Health. *Polish Journal of Environmental Studies*, **32** (1), **2023**.
- POŚNIAK M. Polycyclic aromatic hydrocarbons in the occupational environment during exposure to bitumen fumes. *Polish Journal of Environmental Studies*, **14** (6), **2005**.
- GAJ K., PAKULUK A. Volatile methyl siloxanes as potential hazardous air pollutants. *Polish Journal of Environmental Studies*, **2015**.
- CHRABĄSZCZ M., MRÓZ L. Tree bark, a valuable source of information on air quality. *Polish Journal of Environmental Studies*, **2017**.
- RANINEN K., NENONEN R., JÄRVELÄ-REIJONEN E., POUTANEN K., MYKKÄNEN H., RAATIKAINEN O. Comprehensive two-dimensional gas chromatography-mass spectrometry analysis of exhaled breath compounds after whole grain diets. *Molecules*, **26** (9), **2021**.
- KHATIB M., HAICK H. Sensors for Volatile Organic Compounds. *ACS Nano*, **16** (5), **7080**, **2022**.
- LIN H., JANG M., SUSLICK K.S. Preoxidation for colorimetric sensor array detection of VOCs. *Journal of the American Chemical Society*, **133** (42), **2011**.
- XIA W., HU W., LI Z., YANG J. A first-principles study of gas adsorption on germanene. *Physical Chemistry Chemical Physics*, **16** (41), **2014**.
- SRIMATHI U., NAGARAJAN V., CHANDIRAMOULI R. Germanene nanosheet as a novel biosensor for liver cirrhosis based on adsorption of biomarker volatiles - A DFT study. *Applied Surface Science*, **475**, **2019**.
- KLIMEŠ J., BOWLER D.R., MICHAELIDES A. Chemical accuracy for the van der Waals density functional. *Journal of Physics Condensed Matter*, **22** (2), **2010**.
- RUIZ V.G., LIU W., ZOJER E., SCHEFFLER M., TKATCHENKO A. Density-functional theory with screened van der Waals interactions for the modeling of hybrid inorganic-organic systems. *Physical Review Letters*, **108** (14), **2012**.
- KRILAVICIUTE A., HEISS J.A., LEJA M., KUPCINSKAS J., HAICK H., BRENNER H. Detection of cancer through exhaled breath: A systematic review. *Oncotarget*, **2015**.
- CARRASCO J., SANTRA B., KLIMEŠ J., MICHAELIDES A. To wet or not to wet? dispersion forces tip the balance for water ice on metals. *Physical Review Letters*, **106** (2), **2011**.
- DAVIS J.B.A., BALETTO F., JOHNSTON R.L. The Effect of Dispersion Correction on the Adsorption of CO on Metallic Nanoparticles. *Journal of Physical Chemistry A*, **119** (37), **2015**.
- VO V.O., PHAM T.L., DINH V.A. Adsorption of acetone and toluene on single-vacancy silicene by density

- functional theory calculations. *Materials Transactions*, **61** (8), **2020**.
29. CHETTRI B., PATRA P.K., VU T.V., NGUYEN C.Q., LALRINKIMA YAYA A., OBODO K.O., TRAN N.T.T., LAREF A., RAI D.P. Induced ferromagnetism in bilayer hexagonal Boron Nitride (h-BN) on vacancy defects at B and N sites. *Physica E: Low-Dimensional Systems and Nanostructures*, **126**, **2021**.
30. KHAN K., TAREEN A.K., WANG L., ASLAM M., MA C., MAHMOOD N., OUYANG Z., ZHANG H., GUO Z. Sensing Applications of Atomically Thin Group IV Carbon Siblings Xenon: Progress, Challenges, and Prospects. *Advanced Functional Materials*. **2021**.
31. PETRUSHENKO I.K., PETRUSHENKO K.B. Physical adsorption of N-containing heterocycles on graphene-like boron nitride-carbon heterostructures: A DFT study. *Computational and Theoretical Chemistry*, **1117**, **2017**.
32. HEIMANN J.E., GRIMES R.T., ROSENZWEIG Z., BENNETT J.W. A density functional theory (DFT) investigation of how small molecules and atmospheric pollutants relevant to art conservation adsorb on kaolinite. *Applied Clay Science*, **206**, **2021**.